Quantitative Description of a Protein Fitness Landscape Based on Molecular Features

María-Rocío Meini,[1] Pablo E. Tomatis,[†,1] Daniel M. Weinreich,[2] and Alejandro J. Vila[1,*]

[1]Laboratory of Metalloproteins, Instituto de Biología Molecular y Celular de Rosario (IBR, CONICET-UNR) and Área Biofísica, Facultad de Ciencias Bioquímicas y Farmacéuticas, Universidad Nacional de Rosario, Rosario, Argentina

[2]Department of Ecology and Evolutionary Biology, and Center for Computational Molecular Biology, Brown University

[†]Present address: Biochemisches Institut, Universität Zürich, Zürich, Switzerland

***Corresponding author:** E-mail: vila@ibr-conicet.gov.ar.

Associate editor: Jeffrey Thorne

Abstract

Understanding the driving forces behind protein evolution requires the ability to correlate the molecular impact of mutations with organismal fitness. To address this issue, we employ here metallo-β-lactamases as a model system, which are Zn(II) dependent enzymes that mediate antibiotic resistance. We present a study of all the possible evolutionary pathways leading to a metallo-β-lactamase variant optimized by directed evolution. By studying the activity, stability and Zn(II) binding capabilities of all mutants in the preferred evolutionary pathways, we show that this local fitness landscape is strongly conditioned by epistatic interactions arising from the pleiotropic effect of mutations in the different molecular features of the enzyme. Activity and stability assays in purified enzymes do not provide explanatory power. Instead, measurement of these molecular features in an environment resembling the native one provides an accurate description of the observed antibiotic resistance profile. We report that optimization of Zn(II) binding abilities of metallo-β-lactamases during evolution is more critical than stabilization of the protein to enhance fitness. A global analysis of these parameters allows us to connect genotype with fitness based on quantitative biochemical and biophysical parameters.

Key words: **protein evolution, epistasis, metallo-ß-lactamase, antibiotic resistance.**

Introduction

Protein evolution can be described as a walk on sequence space where a fitness is assigned to each particular sequence, giving rise to the so-called fitness landscape (Smith 1970). Each step on the sequence space represents a mutation, which can exert beneficial, neutral, or deleterious effects on fitness. This fitness landscape can be smooth with a single peak, or rugged with multiple peaks and valleys, depending on the extent of epistatic interactions between mutations (Romero and Arnold 2009; Carneiro and Hartl 2010). Epistasis means that the fitness effect of one mutation depends on the presence or absence of another, that is, on the genetic background where mutations take place. A particular type of epistasis, known as sign epistasis, does not only change the magnitude but also the sign of the fitness effect (Poelwijk et al. 2007). The impact of epistasis in the long-term fixation of mutations is matter of intense debate, including a large amount of theoretical analyses (Breen et al. 2012; McCandlish et al. 2013). Instead, experimental descriptions of epistasis in local fitness landscapes are scarce, despite being essential to understand its impact in protein evolution. A successful approach in this direction is the study of all possible combinations (2^n) of a given set of n mutations, known as combinatorial complete fitness landscape (Weinreich et al. 2013), which helps providing a thorough picture of the multidimensional patterns of epistasis (de Visser et al. 2011). This strategy has been used for a reduced number of systems, providing experimental evidence of epistasis in the following evolutionary models: lysozyme (Malcolm et al. 1990), serine-β-lactamase TEM (Weinreich et al. 2006), isopropylmalate dehydrogenase (Lunzer et al. 2005), sesquiterpene synthetase (O'Maille et al. 2008), dihydrofolate reductase from a malaria parasite (Lozovsky et al. 2009), and deer mouse hemoglobin (Natarajan et al. 2013). Moreover, some of these studies have disclosed how sign epistasis limits the available adaptive pathways to a fitness optima (Weinreich et al. 2006; Lozovsky et al. 2009; Natarajan et al. 2013); that is, those that proceed by accumulation of beneficial mutations.

Protein intragenic epistasis for fitness is thought to arise because of pleiotropic effects of mutations on different protein molecular traits or phenotypes. These traits include but are not limited to: 1) functional phenotypes, such as catalytic activity for enzymes or binding specificity for a transcription factor; and 2) native-fold related phenotypes, like thermodynamic stability and folding, aggregation, and degradation rates (DePristo et al. 2005). The pleiotropic effects of mutations can be well exemplified in the case of resurrected alcohol dehydrogenases from yeast, where mutations changing one kinetic parameters also changed another, reflecting a complex interplay (Thomson et al. 2005). The use of Fisher's geometry model of evolution (Fisher 1958) as a framework for the analysis of pairwise epistasis has provided information about the shape and size of phenotypic space for different examples (Weinreich and Knies 2013). Nevertheless, only a few studies have been able to provide

a complete description of the molecular traits affected by mutations in a combinatorial complete fitness landscape (Lunzer et al. 2005; Natarajan et al. 2013).

A major challenge to understand the biological mechanisms of adaptation is the attempt to correlate genotype with phenotype and fitness at a molecular level (Dean and Thornton 2007). This requires properly addressing the effect of each mutation on different molecular features, accounting for the epistatic phenomena and the pleiotropic effects, which will ultimately determine fitness. Large scale studies of the distribution of fitness effects in the serine-β-lactamase TEM (Jacquier et al. 2013; Firnberg et al. 2014) have been successful in describing the contribution of protein properties to fitness over a large number of mutations. These high-throughput approaches, however, only rely on computational predictions of the thermodynamic stability, due to the difficulties of addressing experimentally this feature over a large number of mutants. Moreover, these analyses have been focused mostly in single mutations, not being able to address the role of epistatic interactions in fitness. Finally, many elegant experimental approaches have addressed the role of epistasis in protein function without pondering the contribution of stability (Lunzer et al. 2005; O'Maille et al. 2008; Natarajan et al. 2013).

Here, we present a study of the evolutionary pathways leading to an optimized enzyme obtained by directed molecular evolution, being able to dissect the contribution of four different mutations, their epistatic interactions and their pleiotropic effects. The model system here employed is a metallo-β-lactamase (MBL), belonging to a family of Zn(II)-dependent enzymes, that have recently emerged as a worrisome problem in the clinical setting (Crowder et al. 2006), outcompeting serine-β-lactamases in some cases (Fisher et al. 2005; Walsh et al. 2011; Meini et al. 2014). Serine-β-lactamases have been successfully employed as model systems for the study of protein evolution (Orencia et al. 2001; Sideraki et al. 2001; Wang et al. 2002; Bershtein et al. 2006; Weinreich et al. 2006; Salverda et al. 2011; Gong et al. 2013). MBLs have an additional constraint for fitness compared to serine-β-lactamases: binding of the Zn(II) cofactor, which is essential for substrate recognition and catalysis (Rasia and Vila 2004; González et al. 2012).

We report the existence of strong sign epistasis for fitness between mutations which influences the available adaptive pathways to the local optimum. When trying to dissect the mechanisms underlying the epistatic interactions in terms of biochemical and biophysical traits, the classical characterization of kinetics and folding stability of purified enzymes failed to describe the effects of mutations on fitness. Instead, quantitation of these features in periplasmic extracts, that is, under conditions mimicking the native environment of the MBLs, allowed us to correlate genotype with phenotypes and fitness. Based on this approach, we provide a quantitative description of the protein fitness landscape based on the biochemical (k_{cat}/K_M) and biophysical traits (stability and Zn(II) binding affinity) affected by each mutation.

Results and Discussion

Epistatic Interactions between Mutations Limit the Number of Adaptive Evolutionary Pathways to a Local Optimum

We have previously obtained an optimized variant of the MBL enzyme BcII from *Bacillus cereus* by directed molecular evolution, which presents four mutations: G262S, L250S, V112A, and N70S; GLVN hereafter (fig. 1*A*) (Tomatis et al. 2005). This variant was selected after four rounds of mutagenesis and selection toward increasing concentrations of cephalexin (a poor wild-type [wt] BcII substrate, see table 1), giving rise to a 2^5-fold increase in the MIC (minimal inhibitory concentration) with respect to wt-BcII (Tomatis et al. 2005).

These four mutations can give rise to $2^4 = 16$ possible mutational combinations in the enzyme BcII. If we assume that mutations accumulate stepwise, there are $4! = 24$ possible pathways to the quadruple mutant. However, if epistatic interactions are present, the probabilities of fixation of each mutation will be different depending on the genetic context, giving rise to distinct accessibility for each trajectory in adaptive evolution (Weinreich et al. 2006).

We now constructed all the aforementioned 16 possible mutational combinations and determined their MIC for cephalexin in *Escherichia coli* cells. MIC values for each variant and the possible mutational trajectories upon accumulation of successive single mutations are shown on figure 1*B*. Mutations G262S and L250S are beneficial when acting on the wt genetic background, because they improve the MIC value from 32 μg/ml to 128 and 64 μg/ml, respectively. In contrast, mutation V112A is neutral and N70S is deleterious on the wt background. A different situation is met when a second mutation is added: L250S, V112A, and N70S are beneficial in the G262S background, all leading to an MIC value of 256 μg/ml. Although there is no epistasis between mutations G262S and L250S, a strong positive epistasis is seen for the cases of G262S/V112A and G262S/N70S. Particularly, in the case of N70S, the sign of the effect changes in G262S background, giving rise to sign epistasis. None of the double combinations between mutations L250S, V112A, and N70S (variants LV, LN, and VN) performs better than wt-BcII. In the case of the triple mutants, any mutation added to a double mutant that includes the G262S mutation leads to MIC values of 512 μg/ml. In contrast, the triple mutant LVN (harboring all mutations except G262S) is not able to provide more resistance than the wt enzyme. Therefore, although mutation L250S is also beneficial in the wt background; G262S stands out as a gateway for evolution, defining the preferred pathways. Finally, the four substitutions (variant GLVN) are required to achieve the maximum level of resistance: 1,024 μg/ml.

Analysis of the MIC values allows us to conclude on the accessibility of the pathways during adaptive evolution. Half of the possible pathways (12 out of 24) are interrupted by a mutation that produces a decrease on MIC (being N70S in ten cases). These pathways are unlikely to occur under strong selection pressure, that is, the conditions that led to the

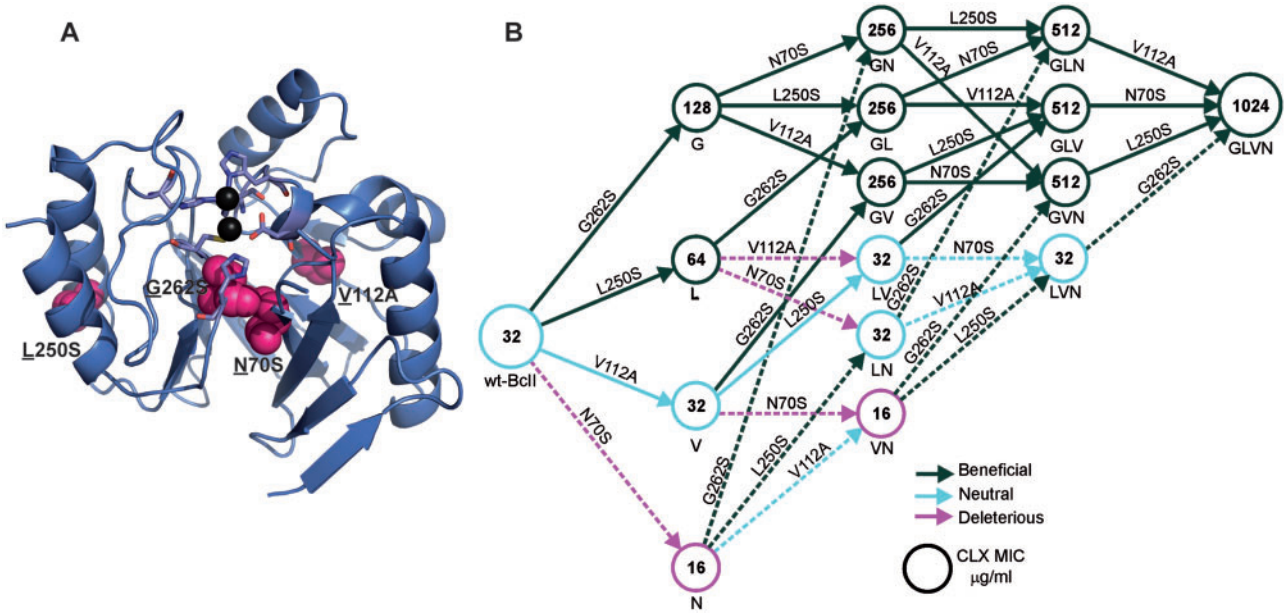

FIG. 1. Structure of the BcII variant GLVN and mutational trajectories from wt-BcII to the evolved mutant GLVN. (*A*) Representation of the GLVN variant structure determined by X-ray crystallography (PDB 3FCZ) (Tomatis et al. 2008). Residues from the active site are shown as sticks, Zn(II) ions as black spheres and sites of mutations as magenta spheres. (*B*) Each combination of the four mutations G262S, L250S, V112A, and N70S was constructed to determine MICs (µg/ml) toward cephalexin conferred to *Escherichia coli*. The letter coding refers to residues from wt-BcII to indicate the presence of each mutation (G stands for G262S, L for L250S, V for V112A, and N for N70S). The single letter coding is used for the protein variant, whereas the two letter-coding including numbering refers to the mutation. MIC values are sequentially ordered according to increasing number of mutations, from wt to the GLVN mutant. Arrows indicate whether the mutation added is beneficial (green), neutral (light blue), or deleterious (light purple) in that genetic background. The circles' colous indicate whether the variant shows an increment (green), no change (light blue), or a decrease (light purple) in the MIC value with respect to wt-BcII. Trajectories including a deleterious mutation are represented by dotted arrows. These are not expected to be successful under strong selection pressure, that is, the conditions that led to selection of mutant GLVN (Tomatis et al. 2005).

optimized variant GLVN (Tomatis et al. 2005). Among the other 12 pathways, 8 are most likely to occur because each step involves a beneficial mutation, 6 of them starting with G262S.

In addition, we analyzed other clones found in the libraries selected at high cephalexin concentration (> 512 µg/ml) on the mentioned directed evolution experiment (Tomatis et al. 2005; supplementary results S1 and table S1, Supplementary Material online) and found that mutations G262S, V112A, and N70S are present in all clones with MIC values of 1,024 µg/ml. These clones also harbor other mutations different from L250S. Therefore, the genetic background of mutant GVN allows several mutations to increase the MIC from 512 to 1,024 µg/ml. Consequently, our results demonstrate that sign epistasis limits the accessible evolutionary pathways to a local optimum and at the same time gives rise to a favorable genetic background for the occurrence of other mutations that diversifies the pathways to alternative optima.

The Catalytic Efficiency of Purified Enzymes Is Insufficient to Describe the Fitness Landscape

To assess the contribution of the catalytic efficiency to MIC values, we purified the eight enzyme variants present in the favored trajectories, that is, those variants including mutation G262S. All eight mutants showed k_{cat}/K_M values toward cephalexin two orders of magnitude higher than wt-BcII (fig. 2*A* and table 1).

We also tested the catalytic efficiency against other β-lactam antibiotics (penicillin G, imipenem, and cefotaxime). Despite the fact that none of these substrates was employed as selection pressure during directed evolution, all variants showed slightly improved hydrolytic rates (2–4 times) compared with the wt enzyme (table 1). Moreover, some variants (G, GN, GVN, and GLVN) showed increased k_{cat}/K_M values by 6-to 20-fold for ceftazidime, which is another poor substrate of wt-BcII. In summary, optimization of cephalexin hydrolysis did not compromise the activity against other substrate but instead, resulted in an expanded substrate profile.

Mutation G262S alone is responsible for the substantial improvement in catalytic efficiency toward cephalexin, a fact that explains the large increment observed in MIC in the case of variant G (fig. 1*B*). However, the catalytic efficiencies of the other variants do not correlate with the successive increases on MICs ($R^2 = 0.24$, fig. 2*B*), failing to account for the enhanced resistance observed upon addition of mutations L250S, V112A, and N70S in the G262S context. These experimental conditions (see supplementary table S2, Supplementary Material online), however, might not reflect the scenario in the bacterial periplasm, where β-lactamases exert their physiological function.

The poor correlation between in vitro and in vivo parameters has been already subject of different studies aimed to

Table 1. Steady-State Kinetic Parameters of wt-BcII and Its Variants toward Different β-Lactam Antibiotics.

Variant	Cephalexin	Cefotaxime	Ceftazidime	Penicillin G	Imipenem
			k_{cat} (s^{-1})		
wt	4 ± 1	100 ± 20	> 25	1,300 ± 70	350 ± 20
G	260 ± 10	400 ± 20	> 160	590 ± 20	56 ± 2
GV	260 ± 10	354 ± 6	ND	1,080 ± 20	68 ± 2
GL	340 ± 8	490 ± 6	ND	1,180 ± 30	118 ± 3
GN	350 ± 10	236 ± 3	> 100	1,300 ± 20	85 ± 2
GLV	340 ± 7	404 ± 5	ND	1,230 ± 30	143 ± 4
GLN	250 ± 6	320 ± 20	ND	980 ± 30	86 ± 3
GVN	300 ± 10	291 ± 4	> 200	1,540 ± 60	73 ± 1
GLVN	360 ± 6	300 ± 5	> 180	1,380 ± 30	94 ± 4
			K_M (μM)		
wt	130 ± 10	43 ± 4	> 1,000	660 ± 70	690 ± 10
G	140 ± 20	54 ± 3	> 1,000	190 ± 10	77 ± 9
GV	110 ± 20	41 ± 3	ND	210 ± 20	71 ± 9
GL	140 ± 10	57 ± 2	ND	220 ± 20	71 ± 6
GN	140 ± 10	37 ± 2	> 300	260 ± 20	42 ± 6
GLV	130 ± 10	66 ± 5	ND	130 ± 10	70 ± 8
GLN	100 ± 9	40 ± 8	ND	230 ± 30	54 ± 7
GVN	120 ± 10	52 ± 3	> 400	380 ± 50	44 ± 5
GLVN	160 ± 10	43 ± 4	> 600	290 ± 30	76 ± 8
			k_{cat}/K_M (μM^{-1} s^{-1})		
wt	0.033 ± 0.004	2.3 ± 0.3	~0.025	1.9 ± 0.2	0.5 ± 0.1
G	1.8 ± 0.3	7.4 ± 1.2	~0.16	3.0 ± 0.4	0.7 ± 0.1
GV	2.3 ± 0.4	8.7 ± 0.8	ND	5.0 ± 0.3	1.0 ± 0.1
GL	2.4 ± 0.2	8.6 ± 0.4	ND	5.5 ± 0.5	1.7 ± 0.2
GN	2.5 ± 0.2	7.5 ± 0.6	~0.30	5.0 ± 0.4	2.0 ± 0.3
GLV	2.5 ± 0.2	6.1 ± 0.5	ND	9.6 ± 0.9	2.0 ± 0.3
GLN	2.6 ± 0.3	7.4 ± 1.4	ND	4.2 ± 0.5	1.6 ± 0.3
GVN	2.5 ± 0.3	5.6 ± 0.3	~0.50	4.1 ± 0.5	1.7 ± 0.2
GLVN	2.2 ± 0.1	7.0 ± 0.6	~0.30	4.7 ± 0.5	1.2 ± 0.1

NOTE.—Reactions were carried out in 10 mM Hepes, pH 7.5, 200 mM NaCl, 20 μM $ZnSO_4$, and 0.05 mg/ml bovine serum albumin at 30 °C. The values shown are the average of at least two independent determinations ± standard error. ND, not determined.

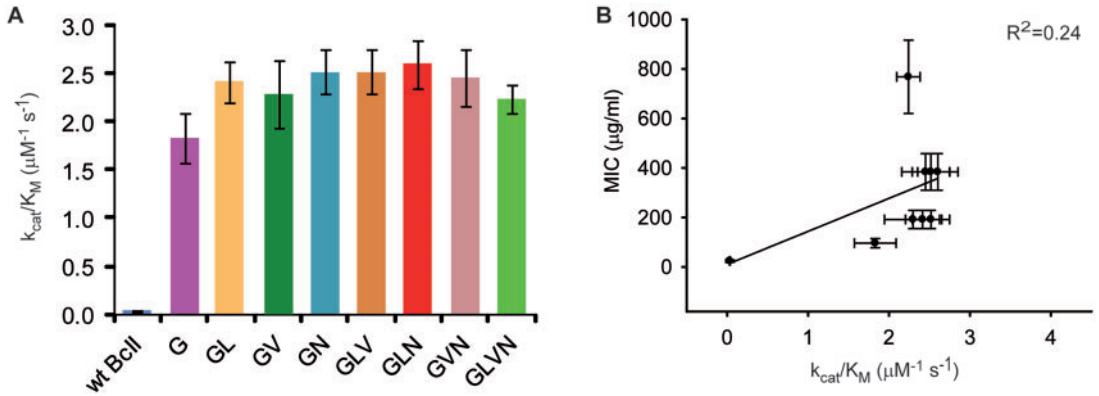

FIG. 2. Catalytic efficiencies determined with purified enzymes. (*A*) Catalytic efficiency toward cephalexin (k_{cat}/K_M) for wt-BcII and its variants determined with purified enzymes. (*B*) MIC values plotted versus k_{cat}/K_M for each variant toward cephalexin.

understand the role of the physiological environment in protein function and structure (Ghaemmaghami and Oas 2001; Ignatova and Gierasch 2004; Ignatova et al. 2007; Gierasch 2011; Latham and Kay 2012, 2013; Sarkar et al. 2013). In many cases, measurements performed in vitro differ substantially from those observed in the cellular context, not only because of the crowding effect but also because of nonspecific weak interactions with other molecules (Latham and Kay

2012, 2013; Sarkar et al. 2013). Remarkably, this approach has not been explored in the study of protein evolution. The accurate quantitation of catalytic efficiencies within the cell is not feasible. Instead, we have recently demonstrated the usefulness of activity measurements in periplasmic extracts as a better correlate of the native conditions (González et al. 2014).

Enzymatic Activities in Periplasmic Extracts Correlate with MIC Values

We obtained periplasmic extracts of *E. coli* cells expressing each of these eight variants (Tomatis et al. 2008). We determined protein concentration of the enzymes on the periplasmic extracts by Western Blot assays employing anti-BcII antibodies and internal calibration curves performed with known quantities of the purified enzymes (fig. 3 and supplementary fig. S1, Supplementary Material online). No significant differences in the protein levels of wt-BcII and the different variants were found on these extracts (fig. 3*B*). We conclude that mutations have not largely affected protein abundance, and so the differences observed in MIC cannot be attributed to that trait.

We then determined the enzymatic parameters toward cephalexin of the different variants in periplasmic extracts aiming to mimic the native environment. Periplasmic extracts were diluted in the same buffer employed to study the activity of purified enzymes, to a similar final protein concentration. Activity measurements with MBLs are routinely performed with excess Zn(II) in the solution and added bovine serum albumin to avoid non-Michaelian behavior that results from protein inactivation due to various processes, including enhanced Zn(II) dissociation in the presence of substrate (González et al. 2012). However, we observed that excess Zn(II) was not required to ensure Michaelian behavior during activity assays performed with enzymes in periplasmic extracts (supplementary fig. S2, Supplementary Material online). Then, activity measurements in these extracts were done without Zn(II) supplementation in order to avoid altering the metal content of the enzymes. Supplementary table S2, Supplementary Material online, summarizes the experimental conditions used in the different activity measurements.

In this way, we estimated apparent k_{cat} and K_M values for the enzymes in the periplasmic extracts (supplementary table S3, Supplementary Material online) from the Michaelis–Menten curves. The resulting picture differs from the one obtained by measuring the activity of purified enzymes. Again, mutation G262S gives rise to a substantial increment in activity compared with the wt enzyme (supplementary table S3, Supplementary Material online), but also the other accumulating mutations further increase the activity (fig. 4*A*). Moreover, MIC values showed a better correlation with $k_{cat}/K_{M\ app}$ parameters determined in periplasmic extracts ($R^2 = 0.68$) (fig. 4*B*); in contrast to the poor correlation observed with data from purified enzymes (fig. 2*B*).

In the case of the serine-β-lactamase TEM-1, it was recently shown that the effects of mutations impact fitness mostly through changes in specific activity rather than perturbing protein abundance (Firnberg et al. 2014). This could be a possible scenario for our model, because mutations do not severely affect protein levels and the purified enzymes activities after mutation G262S do not show substantial differences (fig. 2*A*). Consequently, the discrepancy between purified enzymes and periplasmic extracts data can only be attributed to the existence of distinct fractions of active protein in the native environment. We hypothesized that these levels of active protein reflect changes in the polypeptide stability and/or in the Zn(II) cofactor binding capabilities of the different variants.

Stability Studies in Periplasmic Extracts Identify a Compensatory Stabilizing Mutation

A series of elegant studies in the TEM lactamases (Wang et al. 2002), the HIV protease (Parera et al. 2009), an influenza nucleoprotein (Gong et al. 2013), and DNA gyrase B (Blance et al. 2000) have shown that many mutations eliciting a gain of function are detrimental for the protein stability, therefore reducing the levels of active protein. These deleterious effects are ameliorated by the accumulation of compensatory mutations, which increment fitness by stabilizing the polypeptide. Thermodynamic stability studies employing purified proteins have been of great help in identifying compensatory stabilizing mutations. However, many examples document the inability of these data to properly account for in vivo stabilization (Sideraki et al. 2001; Jacquier et al. 2013).

In order to assess the stability of all mutants in a physiologically relevant context, we devised an assay to probe the thermal stability of all variants in periplasmic extracts. Periplasmic extracts of *E. coli* cells expressing each of the variants were incubated for a fixed time at increasing temperatures and the remaining lactamase activity was measured. The thermal inactivation process was irreversible for all variants. The measured activity values versus the incubation temperature revealed in all cases a sigmoidal behavior that was fit to obtain apparent melting temperatures (T_{Mapp}) (table 2 and supplementary fig. S3, Supplementary Material online). The parameters obtained showed substantial differences between some variants. Mutation G262S is clearly detrimental for protein stability, because it elicits a large decrease in T_{Mapp} (from 71 °C to 61 °C, table 2). Subsequent addition of mutation V112A to the variant G, instead, increases T_{Mapp} to 66 °C (table 2) giving rise to the most stable variant, GV. Similarly, the less stable mutant (GLN, with a T_{Mapp} of 54 °C, table 2) is also stabilized by incorporating mutation V112A. In both cases, addition of mutation V112A results in a larger MIC (fig. 1*B*). V112A behaves as a classical compensatory mutation (Wang et al. 2002; DePristo et al. 2005), restoring stability in different genetic backgrounds. Residue A112 is located in a conserved hydrophobic core in the protein structure, located ca. 15 Å far from G262 (fig.1*A*), suggesting that mutation V112A could act as a global suppressor able to rescue the protein stability (Huang and Palzkill 1997; Bershtein et al. 2008). The effect of V112A constitutes an excellent example

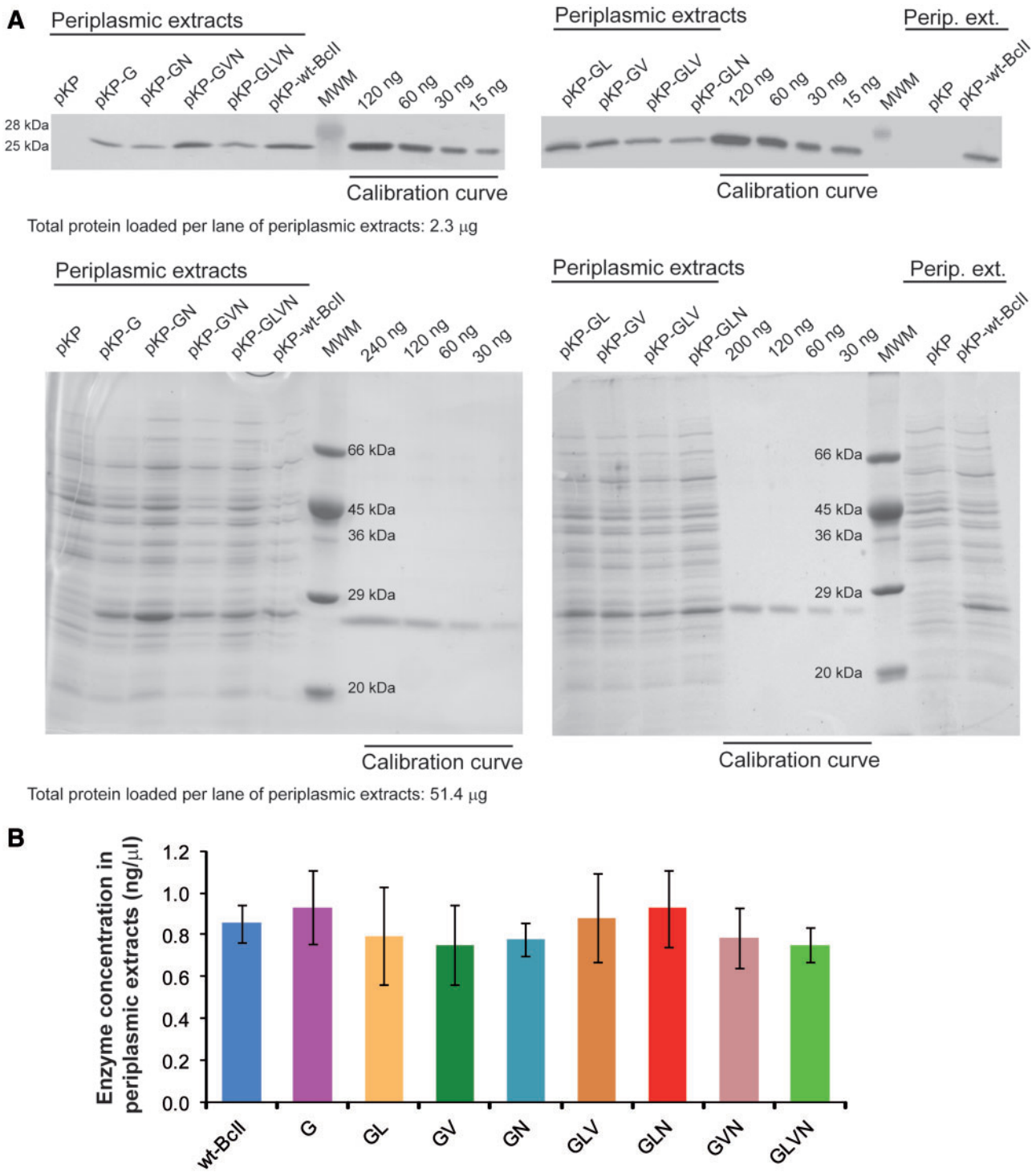

Fig. 3. Quantification of protein abundance in periplasmic extracts by Western Blot analyses. (*A*) Periplasmic extracts of *E. coli* expressing each of the variants as indicated were concentrated 5-fold. The internal calibration curve was performed with known quantities of purified wt-BclI. Enzyme quantity on each band was obtained by densitometry and the response correction factor previously obtained (see supplementary fig. S1, Supplementary Material online) was applied for each variant. MWM: PageRuler Plus Prestained Protein Ladder, Thermo Scientific. For Coomassie visualization extracts were further concentrated 4-fold. MWM, molecular weight markers are indicated in the figure. Total protein concentration was determined with Pierce BCA Protein Assay Kit. (*B*) Protein abundance in periplasmic extracts. The results are the average of three replicates ± standard error. A one way ANOVA test of this data showed that there is no significant difference between the means concentrations for each variant ($P = 0.99$).

of the role of stability-mediated long distance epistatic effect (Lunzer et al. 2010).

In contrast, melting temperatures determined with purified enzymes do not differ considerably among these variants (table 3). As a result, the compensatory role of mutation V112A can only be identified by measurements performed in periplasmic extracts. This fact could be attributed to the destabilizing effect of nonspecific weak interactions in the

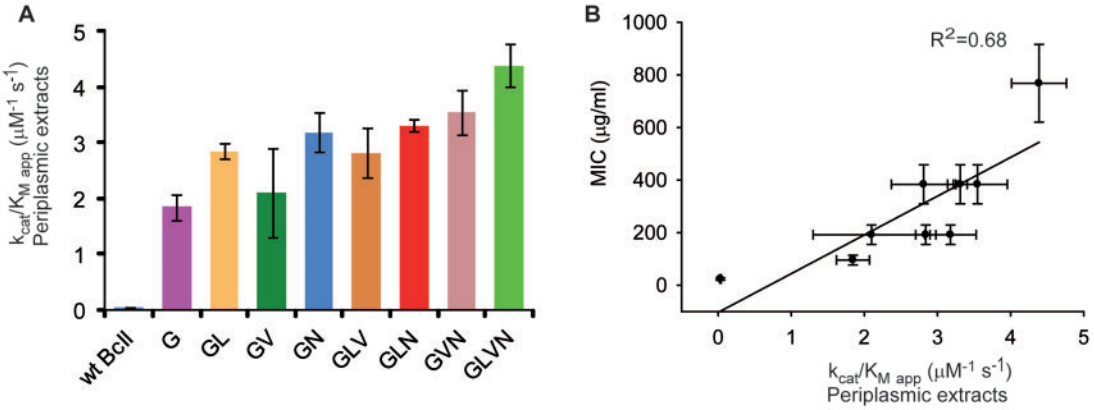

FIG. 4. Catalytic efficiencies determined with periplasmic extracts (*A*) Catalytic efficiency toward cephalexin (k_{cat}/K_M apparent values) for wt-BcII and its variants determined with periplasmic extracts. (*B*) MIC values plotted versus k_{cat}/K_M apparent values determined with periplasmic extracts for each variant toward cephalexin.

Table 2. T_{Mapp} Values Obtained from Thermostability Curves Followed by Activity with Periplasmic Extracts of wt-BcII and Its Variants.

Variant	T_{Mapp} (°C)
wt-BcII	70.7 ± 0.5
G	60.8 ± 0.6
GL	59 ± 2
GV	65.7 ± 0.4
GN	60 ± 2
GVL	58 ± 1
GLN	54.1 ± 0.9
GVN	62 ± 1
GLVN	62 ± 1

NOTE.—T_{Mapp} values shown are the average of at least three experiments performed with independent periplasmic extracts ± the standard error.

Table 3. Comparison of T_{Mapp} Values Obtained from Thermostability Curves Monitored by Different Methods.

Method Variant	T_{Mapp} (°C)		
	Activity in Periplasmic Extracts	Activity of Purified Enzymes	Circular Dichroism at 220 nm
G	60.8 ± 0.6	66.4 ± 0.2	65.6 ± 0.9
GV	65.7 ± 0.4	68.2 ± 0.4	67.9 ± 0.2
GLN	54.1 ± 0.9	63.6 ± 0.6	64.1 ± 0.2
GLVN	62 ± 1	63.9 ± 0.1	64.9 ± 0.3

periplasm (Sarkar et al. 2013), and highlight the importance of testing protein stability in native-like environments. Moreover, the irreversibility of the assays point out that protein inactivation in the periplasmic extracts is governed by kinetic, instead of thermodynamic factors. Kinetic stability describes more accurately the protein behavior in a dynamic and crowded cellular medium, where stability is affected mostly by irreversible processes like degradation and aggregation (Sanchez-Ruiz 2010).

The role of mutations N70S and L250S in protein stability, however, is not evident. These mutations, when operative on the G262S genetic background, elicit MIC enhancements as high as the one induced by V112A (fig. 1*B*) which cannot be attributed to stabilizing effects, based on the T_{Mapp} values (table 2). We conclude that protein stability is not a major factor in describing the fitness increments in all the favored trajectories. However, it is remarkable that the identification of a compensatory stabilizing mutation which explains the epistatic interaction between mutations G262S and V112A could only be accomplished by means of stability measurements in periplasmic extracts.

Cofactor Binding Capabilities Are Selected During Evolution

MBL-mediated resistance to β-lactam antibiotics requires binding of two equivalents of the Zn(II) cofactor in the active site, which is essential for substrate binding and catalysis (Rasia and Vila 2004; Tioni et al. 2008; Tomatis et al. 2008; González et al. 2012). In MBLs, Zn(II) binding takes place in the periplasmic space after translocation of the polypeptide and processing of the signal peptide (Morán-Barrio et al. 2009). *Escherichia coli* is capable of sequestering Zn(II) from the external medium to maintain Zn(II) levels in the cytoplasm even at stringent conditions (Outten and O'Halloran 2001). In the periplasmic space, instead, there is a strong competition for Zn(II) uptake among proteins present in this compartment (Ma et al. 2009) and available Zn(II) depends mostly on the Zn(II) concentration in the external milieu (Hu et al. 2008). In the case of pathogenic bacteria, Zn(II) availability is highly limited in the course of host infection because the host elicits a response, known as "nutritional immunity," during which Zn(II) is sequestered by the protein calprotectin (Kehl-Fie et al. 2011; Brophy et al. 2012). Consequently, Zn(II) binding is crucial for in vivo activation of MBLs.

MBL mutants with low Zn(II) binding affinities give rise to MIC values highly dependent on the Zn(II) concentration in the environment (González JM, et al. 2012; González LJ, et al.

Table 4. MIC Values for Cephalexin in Growth Medium with Different Zn(II) Availability for *Escherichia coli* Cells Expressing wt-BcII or BcII Variants.

	MIC (μg/ml)		
E. coli + pKP-	LB + EDTA 5 μM	LB (15 μM Zn(II))	LB + $ZnSO_4$ 500 μM
—	16	16	16
wt-BcII	16	32	64
G	32	128	512
GL	64	256	1,024
GV	256	256	1,024
GN	256	256	1,024
GLN	512	512	1,024
GLV	512	512	1,024
GVN	512	512	1,024
GLVN	1,024	1,024	1,024

NOTE.—The MICs assays were performed on LB-agar plates containing: EDTA 5 μM, no supplementation and supplemented with $ZnSO_4$ 500 μM.

2014). Therefore, the effect of Zn(II) availability on the MIC values can be exploited as a bona fide indicator of the in vivo Zn(II) binding capabilities of different MBL variants. We determined the effect of Zn(II) availability on antibiotic resistance by measuring cephalexin MIC values for all variants upon addition of the metal chelator ethylenediaminetetraacetic acid (EDTA) or excess Zn(II) (500 μM) to the Luria-Bertani (LB) growth medium (table 4). It is worth mentioning that the variant GLVN was obtained after selection on LB growth medium, which has a Zn(II) concentration of 15 μM.

Antibiotic resistance of cells expressing wt-BcII is sensitive to Zn(II) availability, with MIC values varying between 16 and 64 μg/ml. This sensitivity increases markedly in variant G, whose MICs values span from 32 μg/ml (in the presence of EDTA) to 512 μg/ml (in excess Zn(II)), and decreases as the other three mutations accumulate (table 4). Indeed, the quadruple mutant GLVN is insensitive to changes in the Zn(II) levels, being able to confer a MIC value of 1,024 μg/ml for cephalexin even in the presence of EDTA. These results suggest that these mutations tune the Zn(II) binding affinity of the different variants.

We measured the macroscopic Zn(II) dissociation constant of the two Zn(II) binding events (K_{d1} and K_{d2}) of all five purified variants involved in one of the favored pathways (G-N-GN-GVN-GLVN) by competition binding experiments with the chromogenic chelator 4-(2-pyridylazo)resorcinol (PAR; table 5 and supplementary fig. S4, Supplementary Material online), as previously reported by us (González et al. 2012). Mutations specifically affect the second Zn(II) binding event (K_{d2}), which gives rise to the active di-Zn(II) enzyme. Mutation G262S impairs the Zn(II) binding affinity of the wt enzyme, as reflected by a 20-fold increase in K_{d2} in variant G. The addition of mutation N70S on the G262S background, instead, restores a high Zn(II) binding affinity (variant GN). In contrast, mutation N70S in a wt background does not alter the cofactor affinity (variant N). This pattern parallels the behavior observed in the resistance profile: MIC values of variant G shows a higher sensitivity to Zn(II) availability

Table 5. Macroscopic Zn(II) Dissociation Constants (K_ds) Determined for the Different BcII Variants by Competition Experiments with the Colorimentric Chelator PAR.

	K_{d1} (nM)	K_{d2} (nM)
BcII-wt[a]	<5	9 ± 4
G	4 ± 1	180 ± 50
N	<1	9 ± 2
GN	<0.7	23 ± 5
GVN	2 ± 1	10 ± 2
GLVN	<2	26 ± 5

[a]From (González et al. 2012).

than wt-BcII, which is rescued by addition of mutation N70S (table 4). These results allow us to explain the sign epistasis observed between G262S and N70S by the beneficial effect of G262S on catalytic efficiency toward cephalexin but impaired Zn(II) binding affinity and the restoring effect on Zn(II) binding affinity of N70S mutation in G262S context.

We then measured the activity against cephalexin with periplasmic extracts at various Zn(II) concentration (supplementary fig. S5, Supplementary Material online). These values increase with added Zn(II), reaching a plateau at 1–20 μM Zn(II) (supplementary fig. S5, Supplementary Material online). However, each enzyme variant shows a different behavior. The activity of variant G displays a strong dependence on the Zn(II) concentration in comparison to wt-BcII, and mutants GV, GL, and GLV present a similar behavior. On the other hand, all variants harboring mutation N70S (GN, GLN, GVN, and GLVN) are less sensitive to Zn(II) availability. These results are in agreement with the Zn(II) dissociation constants of the purified enzymes, confirming the detrimental effect of G262S mutations on Zn(II) binding affinity and the compensatory role of N70S. Also, these experiments shed light into the good correlation found in the activity values measured with periplasmic extracts and MICs (fig. 4), because activity measurements without extra Zn(II) added (i.e., before reaching the plateau) do more properly reflects the native metallation state on the periplasma in a nonsupplemented growth medium.

We also tested the effect of Zn(II) availability on the MIC toward other two β-lactams: cefotaxime and ceftazidime (supplementary table S4, Supplementary Material online). We found that the impact of these mutations on Zn(II) dependence behavior show the same trend when the variants are challenged against different substrates. However, the quantitative effect is substrate-dependent, providing a different landscape for selection. For example, though activity against cefotaxime is increased 4-fold by G262S mutation (table 1) it produces a decrease on MIC against cefotaxime from 16 to 2 μg/ml. MIC against this drug is restored by the other mutations or by excess Zn(II) (supplementary table S4, Supplementary Material online). In contrast to the scenario described for cephalexin, mutation G262S would not have been selected against cefotaxime during a directed molecular evolution experiment without the presence of compensatory mutations.

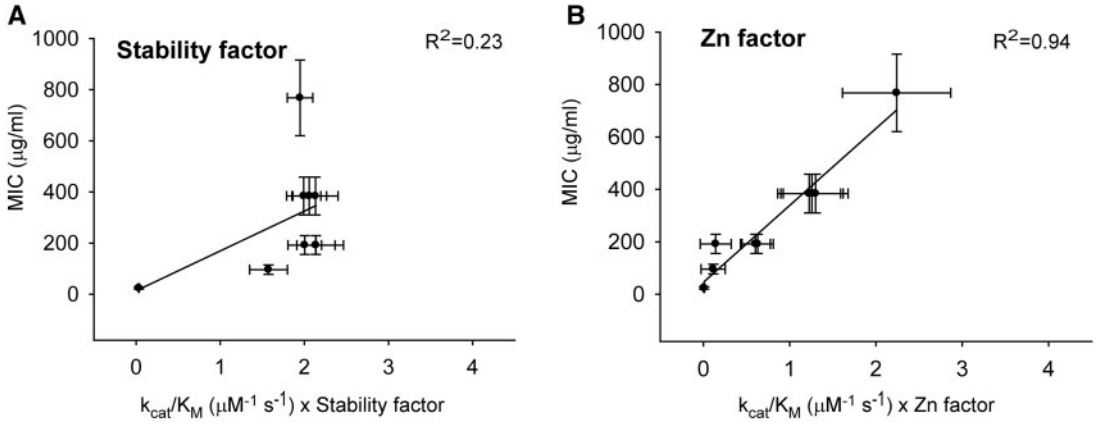

FIG. 5. Correlations between MIC and catalytic efficiency for cephalexin weighed by the contribution of stability and Zn(II) binding affinity. (*A*) MIC values plotted versus k_{cat}/K_M × stability factor; stability factor = $T_{Mapp}{}^{mut}/T_{Mapp}{}^{wt}$ (*B*) MIC values plotted versus k_{cat}/K_M × Zn factor; Zn factor = $MIC_{EDTA}/MIC_{Zn(II)}$.

Overall, these results highlight the pervasive role of Zn(II) binding affinity in defining the fitness landscape of MBLs, which includes strong epistasis between mutations deriving from pleiotropic effects on catalytic parameters and Zn(II) binding affinity.

Quantitative Description of Fitness in Terms of Enzyme Biochemical and Biophysical Features

We modeled the quantitative effect of the molecular features analyzed in shaping organismal fitness. Given that purified enzyme activities do not correlate with the trends in MIC, while measurements performed with periplasmic extracts do, we tested how the analyzed molecular features stability and Zn(II) binding affinity, could account for these differences. We assumed that MIC values are proportional to the catalytic efficiency of the purified enzymes and the amount of active enzyme in the periplasmic space, $[E_{act}]_{peri}$:

$$\text{MIC} \propto \text{catalytic efficiency} \times [E_{act}]_{peri} \quad (1)$$

where $[E_{act}]_{peri}$ depends on the fractions of correctly folded protein and metallated protein. We defined two empiric factors that account for the effects of mutations on these two traits:

$$\text{Stability factor} = T_{Mapp}{}^{mut}/T_{Mapp}{}^{wt} \quad (2)$$

$$\text{Zn factor} = MIC_{EDTA}/MIC_{Zn(II)} \quad (3)$$

Zn factor globally includes the effects observed on K_{ds} and activity dependence on Zn(II) availability, as described in the previous section.

Then, $[E_{act}]_{peri} \propto$ stability factor × Zn factor, which leads to the following equation:

$$\text{MIC} \propto \text{catalytic efficiency} \times \text{stability factor} \times \text{Zn factor} \quad (4)$$

When catalytic efficiencies of the purified enzymes are weighed only by the stability factor, the correlation with MIC values does not improve ($R^2 = 0.23$, fig. 5*A*). Instead, catalytic efficiencies scaled by the Zn factor elicit an excellent correlation ($R^2 = 0.94$, fig. 5*B*). It is evident that the impact of Zn(II) availability in resistance decreases as mutations accumulate in the favored trajectories (table 4), providing a quantitative basis for the role of this factor in the fitness landscape.

Conclusions

The reconstruction of combinatorial complete fitness landscapes provides experimental clues to answer fundamental questions on protein evolution (Weinreich et al. 2013). We have used an in vitro evolved MBL as a model to study protein evolution. This system motivated attention to cofactor binding, an additional dimension to protein activity and stability in our understanding of enzyme evolution. Despite the resulting larger complexity, inclusion of the Zn(II) binding affinity as a biochemical and biophysical trait is essential to properly describe the fitness landscape.

This work reports strong sign epistatic interactions delineating the adaptive pathways of MBLs, in agreement with experimental studies in other model systems (Weinreich et al. 2006; Lozovsky et al. 2009; Natarajan et al. 2013). More importantly, these experiments provide a quantitative framework for the contention that epistasis for fitness derives from pleiotropic mutational effects simultaneously improving one trait while degrading another (DePristo et al. 2005).

The key mutation involved in the interactions with strong sign epistasis, G262S, is responsible for a large increment in the catalytic efficiency, but is detrimental for the enzyme stability and Zn(II) binding affinity. Although we found a stabilizing compensatory mutation (V112A), the polypeptide stability does not globally contribute to explain the changes on MIC upon mutations. Instead, optimization of Zn(II) binding in the periplasm stands as the major component shaping fitness for enzymes with similar catalytic efficiencies. This occurs since mutation N70S on G262S background compensates for the impaired Zn(II) binding affinity, as demonstrated by K_{ds} determinations.

We also report the successful use of activity and stability measurements in periplasmic extracts. Stability data obtained with periplasmic extracts show the advantage of this

approach, which provides a strategy for medium-to-high throughput screening as an experimental alternative to computational predictions on stability in systems with a large number of mutants. Moreover, our data strongly support that the different models of protein evolution should consider kinetic stability in addition to thermodynamic stability for fitness (DePristo et al. 2005). More work in this direction in different systems is clearly needed.

In contrast to activity parameters obtained with purified enzymes, catalytic efficiencies measured with periplasmic extracts show a very good correlation with MIC values. This occurs since in periplasmic extracts the original metallation state is conserved, and provided that Zn(II) is not added to saturation during activity measurements, these are more representative of the enzyme behavior in vivo. In fact, we could weigh the catalytic efficiencies of purified enzymes by considering the Zn(II) binding contribution, obtaining a great improvement in their correlation with MICs. Then, the differences between purified enzymes and periplasmic extracts catalytic efficiencies can be attributed to distinct fractions of active protein in the periplasm. Overall, we conclude that considering biophysical and biochemical factors reporting on the natural environment of the protein allowed us to bridge the gap between in vivo and in vitro results. We foresee that this approach could be exploited to study protein evolution in other systems.

Materials and Methods

Site-Directed Mutagenesis and Plasmids Construction

The different variants with each mutational combination (which are indicated by the original amino acid on wt-BcII) were constructed by site-directed mutagenesis. This was performed by amplification of the entire plasmid using two mutagenic primers and selecting by DpnI digestion. Primers used were 5′-GGTCTACATCGATTGAGAATGTG***TC***GAAGCG ATATAGAAATATAAATGC-3′ and 5′-GCATTTATATTTCTAT ATCGCTTC***GA***CACATTCTCAATCGATGTAGACC-3′ for L250S mutation (the codon is underlined and the mutation is in bold), 5′-GCGTAACGGATG***C***CATTATTACACATGCG***CA*** ***T***GCTGATCGAATTGG-3′and 5′-CCAATTCGATCAG***C*** ***A***TGCG CATGTGTAATAAT***G***GCATCCGTTACGC-3 for V112A mutation and the introduction of SphI restriction site (the codons and the restriction site are underlined and the mutations are in bold). The plasmid pKP (Tomatis et al. 2005) containing the wt *bcII* gene or the mutant *bcII* gene with mutations G262S (variant G), N70S (variant N), or G262S/N70S (variant GN) were used as template to add mutation V112A in order to obtain the genes with the following mutations: V112A (variant V), G262S/V112A (variant GV), V112A/N70S (variant VN), G262S/V112A/N70S (variant GVN).

Plasmids pKP containing the wt or the mutant *bcII* gene of variants G, V, N, GV, GN, and VN were used as templates to add the mutation L250S in order to obtain the genes with mutations: L250S (variant L), G262S/L250S (variant GL), L250S/V112A (variant LV), L250S/N70S (variant LN), G262S/L250S/V112A (variant GLV), G262S/L250S/N70S (variant GLN), and L250S/V112A/N70S (variant LVN).

PCR reactions were performed on a Perkin Elmer Gene Amp PCR System 2400 equipment, with 100 µl reaction mixtures containing 0.3 mM of each dNTP, 0.2 nmol/µl of each primer, $MgSO_4$ 1 mM, 400 ng of the plasmid used as template, 10 µl of the 10× buffer provided with the polymerase, and 2 U of *Pfx* Platinum DNA polymerase (Invitrogen). After an initial step of 30 s at 95 °C, 18 cycles of the following steps were performed: 30 s at 95 °C, 1 min at 55 °C, 5 min at 68 °C followed by a final extension step of 5 min at 68 °C. Template plasmid was digested by the addition of 1 U of DpnI and incubation 1 h at 37 °C and the reaction mixture was then transformed on *E. coli* JM109 cells. The presence of the desired mutations on the DNA plasmid preparation from recovered transformants was corroborated by sequencing (University of Maine Sequencing Facility).

The fragment from the coding region of *bcII* gene was cut with BamHI and XhoI and ligated back into pKP plasmid *lac* or pET-term plasmid. pKP plasmid was used for MIC assays (Tomatis et al. 2005). It contains a promoter for isopropyl β-D-galactopyranoside (IPTG) induction, a leader sequence *pelB* from pectate lyase in order to target the corresponding enzymes to the periplasm and a kanamycin resistance cassette. pET-Term plasmid was used for overexpression (Llarrull, Fabiane, et al. 2007). It contains the complete gene sequence of mature BcII protein as an N-terminal fusion to glutathione-S-transferase (GST) from *Schistosoma japonicas* and the terminator sequence of *bcII* gene. The induction is under control of T7-promoter and the selection is performed with ampicillin. All plasmids sequences used in this work were checked by restriction patterns and DNA sequencing.

Minimal Inhibitory Concentrations

The MICs for cephalexin, cefotaxime, and ceftazidime were determined by the agar dilution method on LB medium. *E. coli* XL1-Blue cells were transformed with pKP plasmid (negative control), or pKP containing the wt *bcII* gene or each of the mutant variants, linked to the leader sequence *pelB* from pectate lyase. Single colonies from each transformation were grown in liquid media overnight (LB with 50 µg/ml kanamycin) at 37 °C with shaking. The saturated cultures were diluted 100 times into fresh media, grown to Optical Density $(OD)_{600\ nm} \sim 0.5$, adjusted to $OD_{600\ nm} = 0.01$, and inoculated with a multiple inoculator with 3-mm inoculating pins on selective media LB agar with 50 µg/ml kanamycin, 0.5 mM IPTG, and variable amounts cephalexin, cefotaxime, or ceftazidime. Alternatively, to determine the influence of Zn(II) availability to MICs, they were determined on LB-medium supplemented with 500 µM $ZnSO_4$ or with 5 µM EDTA added.

Plates were incubated overnight at 37 °C and the MICs were determined form at least three independent experiments. For correlations, we employed the average for the MICs values with their standard error. For tables and figures, the number corresponding to the upper limit was employed to follow the conventional 2-fold dilution series scale.

Protein Expression, Purification, and Sample Preparation

The enzymes wt-BcII and the eight variants of interest (G, GV, GL, GN, GLV, GLN, GVN, GLVN) were expressed using the pET-Term expression vector fused at their N-terminal to GST on the cytoplasm of *E. coli* BL21(DE3)pLysS cells. Induction of expression and purification was performed following the protocol for wt-BcII (Llarrull, Fabiane, et al. 2007). Briefly, overexpression induction was performed at 37 °C for 4 h by addition of IPTG 5 mM. Cells were harvested and resuspended on MTPBS buffer. After cell disruption and ultracentrifugation, the fusion protein GST-BcII was isolated from the crude extract by affinity chromatography employing a glutathione-agarose resine. After that, the fusion was cleaved by thrombin and BcII was isolated from GST by ion exchange chromatography using CM-sepharose resin. All the purification steps were performed at 4 °C, except thrombin treatment that was performed at 26 °C.

Some modifications were necessary because induction of protein overexpression at 37 °C gave rise to unstable and poorly metallated preparations for some of the variants (G, GVN, GLN). In the case of the triple variant GLN, most of the protein was found in the insoluble fractions. Milder induction conditions (20 °C for 16 h) and supplementation with Zn(II) (by adding 500 μM $ZnSO_4$ to the LB medium) gave rise to reproducible and stable protein samples, with acceptable Zn(II) content (1.4-1.8 Zn(II) equivalent per protein molecule) and protein yields (10–15 mg protein/l of culture). In the case of the GLN mutant, these conditions allowed us to obtain sufficient amounts of soluble protein after cells disruption.

Protein samples were quantified spectrophotometrically, using a molar extinction coefficient of 30,500 $M^{-1}cm^{-1}$ (Llarrull, Fabiane, et al. 2007), and their purity was checked by sodium dodecyl sulfate–polyacrylamide gel electrophoresis (SDS–PAGE).

Determination of the Zn(II) content was performed under denaturing conditions using the colorimetric metal chelator PAR as previously described (Fast et al. 2001).

Circular Dichroism spectroscopy was used to test the global folding state of proteins. CD spectrums were performed at the far-UV (200–250 nm) and near UV (250-330 nm) on a Jasco J-810 spectropolarimeter with quartz cuvettes of 0.1 and 1 cm and enzyme concentration of 10 μM and 30 μM respectively, buffer Hepes 10 mM, NaCl 200 mM, pH 7.5, at a constant temperature of 25 °C. As none of the mutations involved aromatic residues, the near UV spectrum represents a fingerprint of the global fold. All variants showed spectra similar to those of wt-BcII, both in the near and far UV (supplementary fig. S6, Supplementary Material online).

Steady-State Kinetic Measurements

Kinetic parameters were determined spectrophotometrically using a Jasco V-680 spectrophotometer following initial reaction rates at different substrate concentrations. To estimate the antibiotic hydrolysis the following differential molar extinction coefficients were used: cephalexin, $\Delta\varepsilon_{266\,nm} = -7{,}800\,M^{-1}cm^{-1}$; cefotaxime, $\Delta\varepsilon_{262\,nm} = -7{,}500\,M^{-1}cm^{-1}$; ceftazidime $\Delta\varepsilon_{262\,nm} = -9{,}000\,M^{-1}cm^{-1}$; imipenem, $\Delta\varepsilon_{300\,nm} = -9{,}000\,M^{-1}cm^{-1}$; and Penicillin G, $\Delta\varepsilon_{235\,nm} = -775\,M^{-1}cm^{-1}$. Reaction medium was 10 mM Hepes pH 7.5, 200 mM NaCl, 20 μM $ZnSO_4$, and 0.05 mg/ml bovine serum albumin at 30 °C.

The plots of the dependence of initial rates on substrate concentration were fitted to the Michaelis–Menten equation using SigmaPlot 8.0. Reported kinetic parameters correspond to the average of at least two determinations with independent protein samples. The k_{cat} values were corrected by the Zn(II) content of the protein samples as previously described (Llarrull, Tioni, et al. 2007). Antibiotics were purchased from SIGMA, with the exception of imipenem and ceftazidime (USP Pharmacopeia). All of them had a purity $> 95\%$.

Periplasmic Extracts

Periplasmic extracts were prepared as previously described (Tomatis et al. 2008; González et al. 2012). Briefly, 5 ml of induced cell culture expressing wt-BcII or BcII variants at $OD_{600nm} = 1$ were washed in 30 mM Tris-HCl, 20 % sucrose buffer (pH 8.0), and then were subjected to osmotic shock with 2 ml of ice-cold 5 mM $MgSO_4$. Considering an average cell volume of 1 μm^3 and that the periplasm represent between 20% and 40% of this volume (Stock et al. 1977), the periplasmic components are diluted ca.1,500-fold on the periplasmic extract assuming a 100% efficiency of the extraction method. These extracts were concentrated 5-fold with Amicon Ultra centrifugal filters MWCO10 kDa and total protein concentration was determined employing Pierce BCA Protein Assay Kit.

SDS–PAGE and Western Blot Assays

From the 5-fold concentrated periplasmic extracts, dilutions were adjusted to load the same protein amount (2.3 μg) on each line of SDS–PAGE 14%. PageRuler Plus Prestained Protein Ladder, Thermo Scientific was employed as molecular weight marker for Western Blots assays. The proteins were transferred to a nitrocellulose membrane and the BcII proteins were identified by rabbit polyclonal antibodies against BcII as described previously (González et al. 2012). In addition, calibration curves were performed with known quantities of purified enzymes in order to evaluate the response of rabbit polyclonal antibodies against wt-BcII for the different variants. Enzyme quantity on each band was obtained by densitometry using GealAnalizer software. Linear response was generally found in the range 0–60 ng. In each case response toward the variant was compared with response toward wt-BcII in the same Western Blot assay. In this way a "correction factor" = wt response/variant response was obtained for each variant, that was later applied to quantified each variant in periplasmic extracts employing an internal wt-BcII calibration curve. The enzyme concentrations on the periplasmic extracts were estimated by densitometry from the corresponding Western Blot band employing an internal wt-BcII calibration curve and the response factors previously determined for each variant.

The results are the average of three replicates ± standard error. After confirming a normal distribution of the residues and equality of variances, a one way analysis of variance (ANOVA) test showed that there is no significant difference between the means concentrations for each variant ($P = 0.99$). These tests were performed with MatLab R2008a software.

Determination of Zn(II) Content by Inductively Coupled Plasma-Mass Spectrometry

In order to determine the total Zn(II) concentration on periplasmic extracts, 0.5 ml of periplasmic extract (at a concentration between 80 and 100 ng/µl of total protein as determined by Pierce BCA Protein Assay Kit) was added to 4.5 ml of 2% nitric acid subboiling quality and ultrapure water. Then, they were injected into the inductively coupled plasma mass spectrometry (ICP-MS) instrument (Agilent 7500 cx). The same procedure was follow with the periplasmic extraction solution ($MgSO_4$ 5 mM), the buffers employed for activity measurements (Hepes 10 mM, NaCl 0.2 M, pH 7.5) untreated and treated with CHELEX-100 to remove Zn(II) traces, and with the LB growth medium. Results are shown on supplementary table S5, Supplementary Material online. These measurements were performed by the ISIDSA service of the Universidad Nacional de Córdoba, Argentina.

Steady-State Kinetic Measurements Performed with Periplasmic Extracts

Initial reaction rates of cephalexin hydrolysis were determined spectrophotometrically at various substrate concentrations employing aliquots from periplasmic extracts of *E. coli* XL1-Blue cells containing wt-BcII or each of the mutant variants. The periplasmic extracts were diluted between 20 and 30 times to obtain final enzyme concentrations on the cuvette between 0.9 and 2 nM (the range usually employed with purified enzymes). Reaction was performed on 10 mM Hepes pH 7.5, 200 mM NaCl at 30 °C. As determined by ICP-MS (see supplementary table S5, Supplementary Material online), the Zn(II) concentration on this buffer solution was 0.16 µM and the maximum extra Zn(II) carried from the periplasmic extract was 0.015 µM.

The plots of the dependence of initial rates on substrate concentration were fitted to the Michaelis–Menten equation using SigmaPlot 8.0.This was repeated at least two times for each variant.

Activity Dependence on Reaction Medium Zn(II) Concentration Measured with Periplasmic Extracts

Reactions were carried out on buffer Hepes 10 mM, NaCl 0.2 M, pH 7.5. First, this solution was extensively stirred with CHELEX-100 in order to remove remaining Zn(II). Then, known quantities of Zn(II) were added from an Standard Spectroscopy Solution of $ZnCl_2$ (SIGMA). As determined by ICP-MS, the concentration of Zn(II) on the untreated buffer was 0.16 ± 0.01 µM and <0.02 µM after treatment with CHELEX-100.

$V_{max\ app}$ values were measured at a cephalexin concentration of 400 µM. Final enzyme concentrations on the cuvette were between 0.9 and 2 nM. For comparison of absolute activities, each $V_{max\ app}$ was divided by the estimated protein concentration ($V_{max\ app}/[E]$). In order to compare the dependence of activity on Zn(II) concentration independently of the activity magnitude, each $V_{max\ app}$ was divided by $V_{max\ app}$ at a concentration of added $[ZnCl_2] = 0$.

Stability Measurements Performed with Periplasmic Extracts

Aliquots of periplasmic extracts from *E. coli* XL1-Blue cells transformed with pKP containing the wt *bcII* gene or each of the eight variants of interest were incubated for five minutes at a fixed temperature between 30 °C and 80 °C and then diluted on the cuvette to measure initial rates as described in the previous section at 30 °C. This was performed with cephalexin in all cases, except for wt-BcII, for which cefotaxime was used (also some curves corresponding to the variants were repeated with cefotaxime and confirmed that they are superimposable to the curves perfomed with cephalexin).

The initial rates from samples incubated at each temperature were divided by the rate corresponding to same sample incubated on ice. In each case, the points were fit to a four parameter sigmoid function with SigmaPlot 8.0 to obtain the apparent transition temperature (T_{Mapp}). These curves were repeated with at least three independent periplasmic preparations.

Stability Measurements Performed by CD Spectroscopy and Activity

Aliquots of purified protein of variants G, GV, GLV, and GLVN (at a concentration of 10 µM on Buffer Hepes 10 mM, NaCl 0.2 M, pH 7.5) were incubated for 5 min at a fixed temperature between 30 °C and 80 °C and then the circular dichroism spectrum was performed at the far-UV region (200–250 nm). The signal at 220 nm was plot against incubation temperature. The same samples were employed to monitor the residual activity and plot it versus incubation temperatures. Reaction medium was 10 mM Hepes pH 7.5, 200 mM NaCl, 20 µM $ZnSO_4$, and 0.05 mg/ml bovine serum albumin at 30 °C. In each case, the points were fit to a four parameter sigmoid function with SigmaPlot 8.0 to obtain the apparent transition temperatures (T_{Mapp}). These curves were repeated with at least two independent preparations.

Zn (II) Binding Affinities Measured by Competition with PAR

Zn(II) binding affinity for BcII mutants G, N, GN, GVN, and GLVN was determined by competition experiments with the chelator PAR as previously described by us (González et al. 2012).

Supplementary Material

Supplementary file S1 is available at *Molecular Biology and Evolution* online (http://www.mbe.oxfordjournals.org/).

Acknowledgments

M.-R.M. was recipient of a doctoral fellowship from Consejo Nacional de Investigaciones Científicas y Técnicas (CONICET). A.J.V. and P.E.T. are Staff members from CONICET. This work was supported by grants from Agencia Nacional de Promoción Científica y Tecnológica (ANPCyT) and the US National Institutes of Health (1R01AI100560) to A.J.V. D.M.W. is supported by grants from the US National Institutes of Health (R01GM095728) and the US National Science Foundation (1038657).

References

Bershtein S, Goldin K, Tawfik DS. 2008. Intense neutral drifts yield robust and evolvable consensus proteins. *J Mol Biol.* 379: 1029–1044.

Bershtein S, Segal M, Bekerman R, Tokuriki N, Tawfik DS. 2006. Robustness-epistasis link shapes the fitness landscape of a randomly drifting protein. *Nature* 444:929–932.

Blance SJ, Williams NL, Preston ZA, Bishara J, Smyth MS, Maxwell A. 2000. Temperature-sensitive suppressor mutations of the *Escherichia coli* DNA gyrase B protein. *Protein Sci.* 9:1035–1037.

Breen MS, Kemena C, Vlasov PK, Notredame C, Kondrashov FA. 2012. Epistasis as the primary factor in molecular evolution. *Nature* 490: 535–538.

Brophy MB, Hayden JA, Nolan EM. 2012. Calcium ion gradients modulate the zinc affinity and antibacterial activity of human calprotectin. *J Am Chem Soc.* 134:18089–18100.

Carneiro M, Hartl DL. 2010. Colloquium papers: adaptive landscapes and protein evolution. *Proc Natl Acad Sci U S A.* 107(Suppl 1), 1747–1751.

Crowder MW, Spencer J, Vila AJ. 2006. Metallo-beta-lactamases: novel weaponry for antibiotic resistance in bacteria. *Acc Chem Res.* 39: 721–728.

de Visser JAGM, Cooper TF, Elena SF. 2011. The causes of epistasis. *Proc Biol Sci.* 278:3617–3624.

Dean AM, Thornton JW. 2007. Mechanistic approaches to the study of evolution: the functional synthesis. *Nat Rev Genet.* 8:675–688.

DePristo MA, Weinreich DM, Hartl DL. 2005. Missense meanderings in sequence space: a biophysical view of protein evolution. *Nat Rev Genet.* 6:678–687.

Fast W, Wang Z, Benkovic SJ. 2001. Familial mutations and zinc stoichiometry determine the rate-limiting step of nitrocefin hydrolysis by metallo-beta-lactamase from *Bacteroides fragilis*. *Biochemistry* 40: 1640–1650.

Firnberg E, Labonte JW, Gray JJ, Ostermeier M. 2014. A comprehensive, high-resolution map of a gene's fitness landscape. *Mol Biol Evol.* 31: 1581–1592.

Fisher JF, Meroueh SO, Mobashery S. 2005. Bacterial resistance to beta-lactam antibiotics: compelling opportunism, compelling opportunity. *Chem Rev.* 105:395–424.

Fisher RA. 1958. The genetical theory of natural selection. New York: Dover.

Ghaemmaghami S, Oas TG. 2001. Quantitative protein stability measurement in vivo. *Nat Struct Mol Biol.* 8:879–882.

Gierasch LM. 2011. A career pathway in protein folding: from model peptides to postreductionist protein science. *Protein Sci.* 20: 783–790.

Gong LI, Suchard MA, Bloom JD. 2013. Stability-mediated epistasis constrains the evolution of an influenza protein. *Elife* 2:e00631.

González JM, Meini MR, Tomatis PE, Medrano Martín FJ, Cricco JA, Vila AJ. 2012. Metallo-β-lactamases withstand low Zn(II) conditions by tuning metal-ligand interactions. *Nat Chem Biol.* 8:698–700.

González LJ, Moreno DM, Bonomo RA, Vila AJ. 2014. Host-specific enzyme-substrate interactions in SPM-1 metallo-β-lactamase are modulated by second sphere residues. *PLoS Pathog.* 10:e1003817.

Hu Z, Gunasekera TS, Spadafora L, Bennett B, Crowder MW. 2008. Metal content of metallo-beta-lactamase l1 is determined by the bioavailability of metal ions. *Biochemistry* 47:7947–7953.

Huang W, Palzkill T. 1997. A natural polymorphism in β-lactamase is a global suppressor. *Proc Natl Acad Sci U S A.* 94:8801–8806.

Ignatova Z, Gierasch LM. 2004. Monitoring protein stability and aggregation in vivo by real-time fluorescent labeling. *Proc Natl Acad Sci U S A.* 101:523–528.

Ignatova Z, Krishnan B, Bombardier JP, Marcelino AMC, Hong J, Gierasch LM. 2007. From the test tube to the cell: exploring the folding and aggregation of a beta-clam protein. *Biopolymers* 88:157–163.

Jacquier H, Birgy A, Nagard HL, Mechulam Y, Schmitt E, Glodt J, Bercot B, Petit E, Poulain J, Barnaud G, et al. 2013. Capturing the mutational landscape of the beta-lactamase tem-1. *Proc Natl Acad Sci U S A.* 110:13067–13072 .

Kehl-Fie TE, Chitayat S, Hood MI, Damo S, Restrepo N, Garcia C, Munro KA, Chazin WJ, Skaar EP. 2011. Nutrient metal sequestration by calprotectin inhibits bacterial superoxide defense, enhancing neutrophil killing of *Staphylococcus aureus*. *Cell Host Microbe* 10: 158–164.

Latham MP, Kay LE. 2012. Is buffer a good proxy for a crowded cell-like environment? A comparative NMR study of calmodulin side-chain dynamics in buffer and *E. coli* lysate. *PLoS One* 7:e48226.

Latham MP, Kay LE. 2013. Probing non-specific interactions of ca^{2+}-calmodulin in *E. coli* lysate. *J Biomol NMR.* 55:239–247.

Llarrull LI, Fabiane SM, Kowalski JM, Bennett B, Sutton BJ, Vila AJ. 2007. Asp-120 locates Zn2 for optimal metallo-beta-lactamase activity. *J Biol Chem.* 282:18276–18285.

Llarrull LI, Tioni MF, Kowalski J, Bennett B, Vila AJ. 2007. Evidence for a dinuclear active site in the metallo-beta-lactamase BcII with substoichiometric Co(II). A new model for metal uptake. *J Biol Chem.* 282:30586–30595.

Lozovsky ER, Chookajorn T, Brown KM, Imwong M, Shaw PJ, Kamchonwongpaisan S, Neafsey DE, Weinreich DM, Hartl DL. 2009. Stepwise acquisition of pyrimethamine resistance in the malaria parasite. *Proc Natl Acad Sci U S A.* 106:12025–12030 .

Lunzer M, Golding GB, Dean AM. 2010. Pervasive cryptic epistasis in molecular evolution. *PLoS Genet.* 6:e1001162.

Lunzer M, Miller SP, Felsheim R, Dean AM. 2005. The biochemical architecture of an ancient adaptive landscape. *Science* 310:499–501.

Ma Z, Jacobsen FE, Giedroc DP. 2009. Coordination chemistry of bacterial metal transport and sensing. *Chem Rev.* 109:4644–4681.

Malcolm BA, Wilson KP, Matthews BW, Kirsch JF, Wilson AC. 1990. Ancestral lysozymes reconstructed, neutrality tested, and thermostability linked to hydrocarbon packing. *Nature* 345:86–89.

McCandlish DM, Rajon E, Shah P, Ding Y, Plotkin JB. 2013. The role of epistasis in protein evolution. *Nature* 497:e1–e2.

Meini MR, Llarrull LI, Vila AJ. 2014. Evolution of metallo-β-lactamases: trends revealed by natural diversity and in vitro evolution. *Antibiotics* 3:285–316.

Morán-Barrio J, Limansky AS, Viale AM. 2009. Secretion of GOB metallo-beta-lactamase in *Escherichia coli* depends strictly on the cooperation between the cytoplasmic Dnak chaperone system and the Sec machinery: completion of folding and Zn(II) ion acquisition occur in the bacterial periplasm. *Antimicrob Agents Chemother.* 53: 2908–2917.

Natarajan C, Inoguchi N, Weber RE, Fago A, Moriyama H, Storz JF. 2013. Epistasis among adaptive mutations in deer mouse hemoglobin. *Science* 340:1324–1327.

O'Maille PE, Malone A, Dellas N, Andes Hess B, Smentek L, Sheehan I, Greenhagen BT, Chappell J, Manning G, Noel JP. 2008. Quantitative exploration of the catalytic landscape separating divergent plant sesquiterpene synthases. *Nat Chem Biol.* 4:617–623.

Orencia MC, Yoon JS, Ness JE, Stemmer WP, Stevens RC. 2001. Predicting the emergence of antibiotic resistance by directed evolution and structural analysis. *Nat Struct Biol.* 8:238–242.

Outten CE, O'Halloran TV. 2001. Femtomolar sensitivity of metalloregulatory proteins controlling zinc homeostasis. *Science* 292: 2488–2492.

Parera M, Perez-Alvarez N, Clotet B, Martínez MA. 2009. Epistasis among deleterious mutations in the HIV-1 protease. *J Mol Biol.* 392:243–250.

Poelwijk FJ, Kiviet DJ, Weinreich DM, Tans SJ. 2007. Empirical fitness landscapes reveal accessible evolutionary paths. *Nature* 445:383–386.

Rasia RM, Vila AJ. 2004. Structural determinants of substrate binding to *Bacillus cereus* metallo-beta-lactamase. *J Biol Chem.* 279: 26046–26051.

Romero PA, Arnold FH. 2009. Exploring protein fitness landscapes by directed evolution. *Nat Rev Mol Cell Biol.* 10:866–876.

Salverda MLM, Dellus E, Gorter FA, Debets AJM, van der Oost J, Hoekstra RF, Tawfik DS, de Visser JAGM. 2011. Initial mutations direct alternative pathways of protein evolution. *PLoS Genet.* 7: e1001321.

Sanchez-Ruiz JM. 2010. Protein kinetic stability. *Biophys Chem.* 148: 1–15.

Sarkar M, Smith AE, Pielak GJ. 2013. Impact of reconstituted cytosol on protein stability. *Proc Natl Acad Sci U S A.* 110:19342–19347.

Sideraki V, Huang W, Palzkill T, Gilbert HF. 2001. A secondary drug resistance mutation of tem-1 beta-lactamase that suppresses misfolding and aggregation. *Proc Natl Acad Sci U S A.* 98:283–288.

Smith JM. 1970. Natural selection and the concept of a protein space. *Nature* 225:563–564.

Stock JB, Rauch B, Roseman S. 1977. Periplasmic space in *Salmonella typhimurium* and *Escherichia coli*. *J Biol Chem.* 252: 7850–7861.

Thomson JM, Gaucher EA, Burgan MF, de Kee DW, Li T, Aris JP, Benner SA. 2005. Resurrecting ancestral alcohol dehydrogenases from yeast. *Nat Genet.* 37:630–635.

Tioni MF, Llarrull LI, Poeylaut-Palena AA, Martí MA, Saggu M, Periyannan GR, Mata EG, Bennett B, Murgida DH, Vila AJ. 2008. Trapping and characterization of a reaction intermediate in carbapenem hydrolysis by *B. cereus* metallo-beta-lactamase. *J Am Chem Soc.* 130:15852–15863.

Tomatis PE, Fabiane SM, Simona F, Carloni P, Sutton BJ, Vila AJ. 2008. Adaptive protein evolution grants organismal fitness by improving catalysis and flexibility. *Proc Natl Acad Sci U S A.* 105: 20605–20610.

Tomatis PE, Rasia RM, Segovia L, Vila AJ. 2005. Mimicking natural evolution in metallo-beta-lactamases through second-shell ligand mutations. *Proc Natl Acad Sci U S A.* 102:13761–13766.

Walsh TR, Weeks J, Livermore DM, Toleman MA. 2011. Dissemination of NDM-1 positive bacteria in the New Delhi environment and its implications for human health: an environmental point prevalence study. *Lancet Infect Dis.* 11:355–362.

Wang X, Minasov G, Shoichet BK. 2002. Evolution of an antibiotic resistance enzyme constrained by stability and activity trade-offs. *J Mol Biol.* 320:85–95.

Weinreich DM, Delaney NF, Depristo MA, Hartl DL. 2006. Darwinian evolution can follow only very few mutational paths to fitter proteins. *Science* 312:111–114.

Weinreich DM, Knies JL. 2013. Fisher's geometric model of adaptation meets the functional synthesis: data on pairwise epistasis for fitness yields insights into the shape and size of phenotype space. *Evolution* 67:2957–2972.

Weinreich DM, Lan Y, Wylie CS, Heckendorn RB. 2013. Should evolutionary geneticists worry about higher-order epistasis? *Curr Opin Genet Dev.* 23:700–707.